J. Math. Biol. (2013) 66:1209–1240
DOI 10.1007/s00285-012-0530-0

Mathematical Biology

A model of erythropoiesis in adults with sufficient iron availability

Doris H. Fuertinger · Franz Kappel · Stephan Thijssen · Nathan W. Levin · Peter Kotanko

Received: 2 October 2011 / Revised: 31 March 2012 / Published online: 18 April 2012

Abstract In this paper we present a model for erythropoiesis under the basic assumption that sufficient iron availability is guaranteed. An extension of the model including a sub-model for the iron dynamics in the body is topic of present research efforts. The model gives excellent results for a number of important situations: recovery of the red blood cell mass after blood donation, adaptation of the number of red blood cells to changes in the altitude of residence and, most important, the reaction of the body to different administration regimens of erythropoiesis stimulating agents, as for instance in the case of pre-surgical administration of Epoetin-α. The simulation results concerning the last item show that choosing an appropriate administration regimen can reduce the total amount of the administered drug considerably. The core of the model consists of structured population equations for the different cell populations which are considered. A key feature of the model is the incorporation of neocytolysis.

Keywords Erythropoiesis · Neocytolysis · Structured population models

Mathematics Subject Classification 92C30 · 92D25 · 35Q92

D. H. Fuertinger · F. Kappel (✉)
Institute for Mathematics and Scientific Computing, University of Graz, Graz, Austria
e-mail: franz.kappel@uni-graz.at

D. H. Fuertinger
e-mail: doris.fuertinger@edu.uni-graz.at

S. Thijssen · N. W. Levin · P. Kotanko
Renal Research Institute New York, New York, USA
e-mail: sthijssen@rriny.com

N. W. Levin
e-mail: nlevin@rriny.com

P. Kotanko
e-mail: PKotanko@rriny.com

1 Introduction

In 2006 around 1.4 million patients received dialysis treatment with an estimated growth to 2.0 million in 2010. Of these treatments approximately 21 % took place in the US and 17 % in the EU (see Kotanko et al. 2007). These numbers will increase strongly in the future. Almost all patients with chronic kidney disease are affected by chronic anemia which is mainly caused by failure of renal excretory and endocrine function. Erythropoietin (EPO), the hormone which drives the production of new red blood cells, is primarily produced in the kidneys (and only in an insufficient amount in the liver). Anemia not only reduces physical and neurocognitive capacity and worsens quality of life, but it also leads to left ventricular hypertrophy, left ventricular dilation, and myocardial ischemia. These adaptive cardiovascular compensation mechanisms, which try to maintain sufficient oxygen supply for the tissues, are risk factors for cardiovascular disease and death (Strippoli et al. 2004). Partial correction of anemia in dialysis patients reduces cardiovascular mortality, which is the most common cause of death among these patients (Besarab et al. 1998; Go et al. 2004). Erythropoiesis stimulating agents (ESA) exert hematological effects analogous to those of EPO. ESA treatment regimens (administered doses and frequency of administration) are usually determined based on the prior experience of the physician and on established guidelines, because predictive models of erythropoiesis under an ESA treatment regimen are not readily available. The model presented in this paper introduces such a predictive model of erythropoiesis taking ESA administration into account.

There exist several mathematical models of erythropoiesis in the literature. Many of them were inspired by the model described in Belair et al. (1995). This model consists of two partial differential equations, one describing the cells in the bone marrow committed to the erythroid cycle, and the second one describing the red blood cell (RBC) population circulating in the peripheral blood. The authors assumed that EPO influences the recruitment of pluripotent stem cells into the erythroid lineage and the proliferation of precursor cells in the bone marrow. This model has been modified and analyzed several times and fitted to different experimental data from different authors. For example, an improved version of this model was published by Mahaffy et al. (1998). The authors added an EPO dependent rate of apoptosis of precursor cells and introduced a moving boundary condition for mature erythrocytes. This condition allows for a variable maximal life span of RBC. They fitted the model to experimental data of rabbits suffering from an induced auto-immune hemolytic anemia. The same model was later also fitted to experimental data for phlebotomy in humans (see Mahaffy et al. 1999). The work presented in Adimy et al. (2006) is also inspired by the paper of Belair et al. and considers an application to periodic hematological diseases. Recently, Crauste et al. (2008) added another modification to the "Belair" model (self-renewal of progenitor cells). A theoretical analysis of the Belair model and of some of its modifications can be found, for example, in Ackleh et al. (2002, 2006) and in Banks et al. (2004).

Another important contribution to modeling of erythropoiesis was presented by Loeffler and his collaborators (see e.g., Loeffler et al. 1989; Wichmann et al. 1989; Wulff et al. 1989). In more recent publications (see e.g., Roeder and Loeffler 2002; Roeder 2006) the focus is primarily on modeling of the hematopoietic stem cells and not as much on erythropoiesis itself.

So far, none of the models discussed above was used or designed for predicting a patient's erythropoietic response to ESA administration. The model presented in the following sections differs distinctly in some aspects from erythropoiesis models published up to now. The model is more detailed concerning the stages a cell has to pass through in its development from a stem cell to an erythrocyte. We distinguish four stages in the development of cells committed to the erythroid lineage in bone marrow and one describing red blood cells circulating in blood. Another important feature is that in case of mature erythrocytes we account for a mechanism called neocytolysis, which was only recently found to contribute to renal anemia and also seems to trigger active destruction of young RBCs (neocytes) in other situations when EPO is administered (see Chang et al. 2009; Rice et al. 1999). Adding this mechanism to the model proved to be crucial to fit experimental data well.

The mathematical model developed in this paper proves to be valid for a wide range of situations. It is able to describe the recovery of the RBC mass after blood donation, the reaction of the body to pre-surgical administration of Epoetin-α and the changes in the number of erythrocytes in high altitude dwellers descending to sea level. Concerning dialysis patients, it is only applicable for a small group. This is because one of the assumptions for the model presented here, is that the body is able to provide sufficient iron supply for erythropoiesis at all times. As 80–90 % of dialysis patients treated with ESA suffer from functional iron deficiency at some stage in their therapy (Schaefer and Schaefer 1998), this assumption is only valid for a minority of dialysis patients. An extension of the model presented here incorporating a comprehensive sub-model for iron homeostasis is a topic of present and future research and has the goal to expand the possible applications to the majority of dialysis patients and to pathologies where unbalanced iron homeostasis leads to abnormal erythropoiesis (e.g., absolute and functional iron deficiency anemia, haemochromatosis, etc.).

In the next section we present the basic physiological facts which are necessary to follow the development of the mathematical model in Sect. 3. In Sect. 4 we give a short description of the numerical algorithm used for the simulations. Section 5 contains the simulation results for the following concrete situations:

- Adaptation of the number of erythrocytes in high altitude dwellers, when they move for longer periods to lower altitudes.
- Recovery of the RBC mass after a blood donation.
- Pre-operative EPO administration.

Section 5 further contains some theoretical simulations. We compare our model to experimental data in different situations and see, by using the same parameter values for all simulations, a very satisfying qualitative and quantitative behavior of the model throughout the simulations.

2 Regulation of erythropoiesis

In the following we present some basic facts on erythropoiesis which are used in Sect. 3. For details and an excellent overview of erythropoiesis we refer to Greer et al. (2009), Lichtman et al. (2005).

RBCs (erythrocytes) are essential for the distribution of oxygen to organs and tissues in the body. They take up oxygen in the lungs and deliver it to tissues while squeezing through the capillaries. To fulfill this task properly they are highly specialized. They are shaped like biconcave disks in order to optimize oxygen exchange and give up their nuclei, organelles and mitochondria in order to provide more space for hemoglobin, the molecule which binds oxygen. Erythrocytes are very deformable and can therefore pass capillaries half their diameter. They withstand a high shear stress, rapid elongation, folding and deformation during their passage through the microcirculation. Over time the cell membrane is damaged by these extraordinary stresses. Because of the lack of nuclei and organelles, red blood cells cannot divide or repair their cell membranes. Senescent erythrocytes lose their flexibility due to their fragmented membranes. These stiff cells could do harm to small capillaries or even clog them. To avert this, old erythrocytes are recognized by phagocytes and destroyed. This phagocytosis mainly takes place in the spleen (Jandl 1987).

To compensate for phagocytosis of senescent red blood cells it is necessary to build new erythrocytes continuously. The maturation of undifferentiated stem cells to mature erythrocytes is called erythropoiesis and takes place in the bone marrow. Erythropoiesis does not only have to account for the loss of old erythrocytes but also for the additional loss of cells due to random breakdown as well as due to internal and external bleeding. Furthermore, the number of RBCs has to be adjusted to varying environmental conditions, as for instance a transition from low to high altitudes or vice versa, by increasing the rate of erythropoiesis, or, conversely, by starting neocytolysis, a process believed to involve macrophages in order to phagocytose young erythrocytes (neocytes) (Alfrey and Fishbane 2007; Chang et al. 2009; Rice and Alfrey 2005; Udden et al. 1995).

During the process of erythrocyte development, a cell undergoes a series of proliferations and differentiations. Starting from multi-potent stem cells, erythroid cells mature to burst-forming unit erythroids (BFU-E) (earliest stage of cells committed to the erythroid lineage), colony-forming unit erythroids (CFU-E), different stages of erythroblasts and finally reticulocytes. The reticulocytes are released from bone marrow into blood and mature in 1–3 days to erythrocytes (see Fig. 1).

The primary control of erythropoiesis is governed by the hormone erythropoietin (EPO). EPO is released into the blood stream by the kidneys based on a negative feedback mechanism that reacts to the partial pressure of oxygen in blood. The concentration of EPO affects the number of circulating red blood cells by determining the rate at which cells mature into erythrocytes either by recruitment or by preventing apoptosis (programmed cell death) and by affecting the maturation velocity of progenitor and precursor cells. Thus, changes in oxygen delivery can be adapted to the needs by an adaptive resetting of the rate of erythropoiesis. Additionally, as already mentioned above, the process of neocytolysis, which affects the selective degradation of young erythrocytes, is activated in situations of red cell excess. Neocytolysis seems to be triggered by a drop in the EPO level (Alfrey and Fishbane 2007; Rice et al. 1999, 2001).

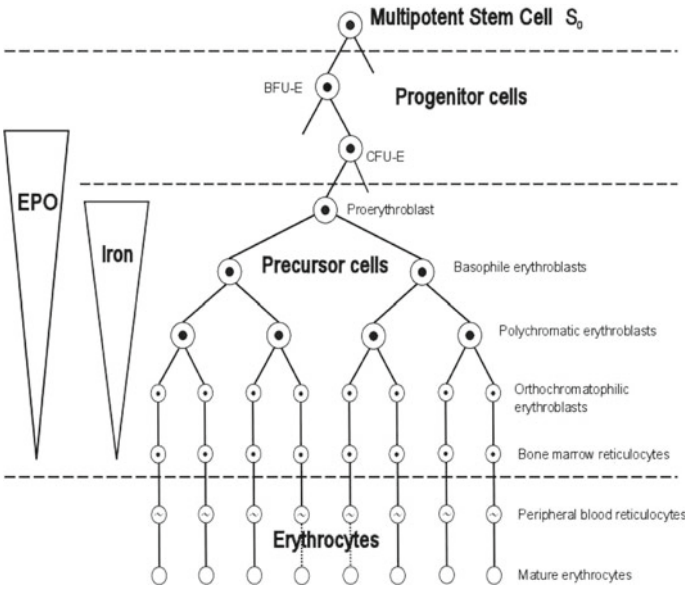

Fig. 1 Diagram of the different cell stages during erythropoiesis. The changing width of the *triangles* labeled "EPO" and "IRON" represents the receptor densities on the cells

Another critical factor for effective erythropoiesis is iron, which is indispensable for hemoglobin synthesis. If the body is not able to provide sufficient iron for this process, then ineffective erythropoiesis will result (Finch et al. 1950; Lichtman et al. 2005). In normal subjects, the total iron content of the body remains within narrow limits. Once an atom of iron enters the body it is conserved with remarkable efficiency and can remain in the body for more than ten years. Iron is only lost via loss of cells (especially intestinal epithelial cells), bleeding and loss of very small amounts via urine and sweat. The balance of iron content is achieved by controlling absorption and not by control of excretion. If the concentration of iron in plasma and/or in the iron stores is too low, then the level of the hormone hepcidin is decreased. The consequence of a lower hepcidin level is that more iron is taken up via the duodenum and more iron is released from macrophages and from storage (Crichton 2009; Fleming 2008). Hepcidin release is also activated by inflammation, which is a prominent problem in chronic kidney disease. Hepcidin is an acute phase-reactant and during inflammation its production in the liver is increased. An elevated hepcidin level partly or fully blocks the release of iron from stores and the reticuloendothelial system as well as absorption of dietary iron in the intestine. Thus, the body is not able to sufficiently supply developing red blood cells with iron and, as a consequence, erythropoiesis is impaired.

3 A model of erythropoiesis in adults with normal RBC lifespan and adequate iron availability

The model of erythropoiesis in humans presented in this paper is based on structured population models for the different cell stages. Since individual cells in the various

cell populations which are considered are distinguished by their maturity, which is also often referred to as cell age, we used so called age-structured population models in order to describe the development of the cell populations. Besides the equations for these age-structured population classes, the model includes a feedback loop representing the actions of EPO. In the present model, we did not account for impaired erythropoiesis due to iron deficiency, but instead choose a constant rate of ineffective erythropoiesis (i.e., a constant baseline apoptosis rate during erythropoiesis), which is seen in healthy persons without iron deficiency.

The different cell types are grouped into population classes according to their characteristic properties during erythropoiesis with respect to interaction with EPO and iron. These properties concern the proliferation rate, the rate of apoptosis and the maturation velocity of cells, which—depending on the type of cell—may change depending on erythropoietin and/or iron levels. Five different population classes of cells are considered: BFU-E, CFU-E, erythroblasts, marrow reticulocytes and erythrocytes (including blood reticulocytes).

For each population class listed above, a model of the type

$$\frac{\partial}{\partial t}u(t,\mu) + v(E(t))\frac{\partial}{\partial \mu}u(t,\mu) = \Big(\beta(E(t)) - \alpha(E(t), z(t), \mu)\Big)u(t,\mu) \qquad (1)$$

is developed, where $u(t,\cdot)$ is the population density with respect to the attribute maturity μ at time t, i.e., $\int_{\mu_1}^{\mu_2} u(t,\mu)\,d\mu$ is the number of cells with maturity $\mu \in [\mu_1, \mu_2]$. Furthermore, $\beta(\cdot)$ and $\alpha(\cdot)$ describe proliferation rate and the rate of apoptosis (mortality), respectively, of the cell populations. These functions depend a priori on the maturity μ and the concentrations $E(t)$ and $z(t)$ of EPO and iron, respectively, at time t. The function $v(\cdot)$ describes the maturation velocity and may depend on the concentration $E(t)$.

The commitment to the erythroid lineage is an irreversible event. A differentiated cell cannot regress or switch to another differentiation pathway. Thus, once a multi-potent stem cell has committed to the erythroid lineage, it undergoes the complete series of differentiations until it becomes a red blood cell or it dies during this process. While maturing, the cell changes its characteristics (e.g., reduction in size, number of transferrin or EPO receptors, decrease in the amount of RNA/DNA etc.). The process of how stem cells are recruited into the proliferating progenitor population remains unclear. There are several hypotheses including an environmental dependency, a random event, etc. In the following we refer to committed erythroid cells in the bone marrow as progenitor (BFU-E and CFU-E cells) and precursor cells (from pro-erythroblasts to marrow reticulocytes).

3.1 Progenitor cells: BFU-E and CFU-E cells

Assumptions

1. The rate at which cells commit to the erythroid lineage is constant.
2. Cells stay in this stage for 13 days (7 days BFU-E and 6 days CFU-E).

3. The number of transferrin receptors on BFU-E and CFU-E is negligible, i.e., iron has no influence on progenitor cells.
4. EPO has no effect on the number of BFU-E, i.e., the proliferation rate for BFU-E cells is constant.
5. The apoptosis rate of BFU-E is zero.
6. The proliferation rate for CFU-E cells is constant.
7. The rate of apoptosis for CFU-E cells depends strongly on the EPO concentration in plasma.
8. The maturation velocities of BFU-E and CFU-E cells are constant and assumed to be one.

The earliest identifiable erythroid progenitor cell is the BFU-E. Morphologically it is difficult to identify. Moreover, a distinction between BFU-E and the next cell stage—CFU-E—is valid but to some extent artificial. There are cells in between these two developmental stages which show characteristics between BFU-E and CFU-E. In culture it lasts around 6–7 days until human BFU-E have all the functional characteristics of CFU-E (Lichtman et al. 2005). Early BFU-E have only a very small number of EPO- and transferrin-receptors (Greer et al. 2009). They are totally dependent on interleukin-3 for their survival, but EPO has no effect on proliferation or apoptosis of these cells (Wu et al. 1995).

The colony-forming unit erythroid (CFU-E) is a more differentiated type of progenitor cell. CFU-E are rapidly dividing cells compared to the slower-dividing BFU-E (Wu et al. 1995). They have a large number of EPO receptors and are strongly dependent on EPO for their survival, i.e., the rate of apoptosis depends on EPO. Under normal conditions, large numbers of generated CFU-E do not survive (Greer et al. 2009). CFU-E cells still have only a few transferrin receptors. Since transferrin receptors are responsible for the uptake of iron, it is reasonable to neglect the influence of iron on all types of progenitor cells.

Let $p(t, \mu^p)$ denote the population density for the BFU-E, where μ^p is the maturity of a BFU-E cell which, according to Assumption 8, coincides with the age of the cell. In view of our assumptions, we get the following model equations for the BFU-E population:

$$\begin{aligned} \frac{\partial}{\partial t} p(t, \mu^p) + \frac{\partial}{\partial \mu^p} p(t, \mu^p) &= \beta^p p(t, \mu^p), \\ p(t, 0) &= S_0, \\ p(0, \mu^p) &= p_0(\mu^p), \end{aligned} \tag{2}$$

where β^p is a constant proliferation rate (Assumption 4), S_0 describes the constant rate at which stem cells commit to the erythroid lineage (Assumption 1, note also that μ^p has the dimension of time and consequently p_0 has the dimension 1 over time), $p_0(\mu^p)$ is the population density at $t = 0$ with $0 \leq \mu^p \leq \mu^p_{\max} = 7$ (Assumption 2), and $t \geq 0$.

CFU-E with population density $q(t, \mu^q)$ are considered separately. Once a BFU-E cell reaches the maximum age for BFU-E cells it leaves this class and becomes a CFU-E cell, i.e., there is a flux of cells from one population class to the next one.

Let $\mu^q \to q(t, \mu^q)$ be the population density for CFU-E cells, where μ^q is the maturity of these cells which coincides with the age (Assumption 7). We get the following model equations for the CFU-E cell population:

$$\begin{aligned} \frac{\partial}{\partial t} q(t, \mu^q) + \frac{\partial}{\partial \mu^q} q(t, \mu^q) &= \left(\beta^q - \alpha^q(E(t))\right) q(t, \mu^q), \\ q(t, \mu^q_{\min}) &= p(t, \mu^p_{\max}), \\ q(0, \mu^q) &= q_0(\mu^q), \end{aligned} \tag{3}$$

where β^q is the constant proliferation rate (Assumption 6), $\alpha^q(E(t))$ denotes the rate of apoptosis depending on the EPO concentration in plasma (Assumption 7), $q(t, \mu^q_{\min}) = p(t, \mu^p_{\max})$ describes the number of cells leaving the BFU-E cell stage and entering the CFU-E cell stage, $q_0(\mu^q)$ is the population density at $t = 0, 7 = \mu^q_{\min} \leq \mu^q \leq \mu^q_{\max} = 13$ (Assumption 2), and $t \geq 0$.

We use a sigmoid function to describe the apoptosis rate $\alpha^q(E(t))$,

$$\alpha^q(E(t)) = \frac{a_1 - b_1}{1 + e^{k_1 E(t) - c_1}} + b_1, \tag{4}$$

where $E(t)$ is the EPO concentration at time t. The function monotonically decreases with increasing EPO concentration. Thus, a higher level of EPO causes more cells to survive.

3.2 Precursor cells: erythroblasts and marrow reticulocytes

Assumptions

9. Cells stay in this stage for 6–8 days (5 days erythroblasts and 1–3 days marrow reticulocytes).
10. The class of erythroblasts consists of all cell stages from proerythroblast to orthochromatophilic erythroblast.
11. Proliferation of erythroblasts is assumed to be constant.
12. The maturation velocity of erythroblasts is constant and assumed to one.
13. The maturation velocity of reticulocytes depends on the EPO concentration in plasma.
14. Reticulocytes do not proliferate.
15. Even with sufficient iron supply, a constant fraction of marrow reticulocytes is phagocytosed per unit time.

After a CFU-E has differentiated into a proerythroblast, it takes about another 6–8 days until the cell is released from the bone marrow into the bloodstream (Jandl 1987). The various stages of maturation from proerythroblast to orthochromatophilic erythroblast (see Fig. 1) are referred to as erythroblasts. The cells undergo several mitotic divisions until at the stage of orthochromatic erythroblast they lose their ability to divide and enter a maturation period. During this time, the cell expels its nucleus and is called a reticulocyte. The erythroblastic pyramids appear normal, with no evidence

of additional mitotic divisions, when production increases, i.e., we assume proliferation of erythroblasts to be constant (Lichtman et al. 2005).

The precursor cells are EPO- and iron-sensitive. While EPO receptors decline during the differentiation from erythroblasts to reticulocytes, transferrin-receptors increase sharply in the early erythroblast forms and reach their peak in intermediate erythroblasts before slowly declining again (Greer et al. 2009), thus reflecting the increased demands of the cells for iron to synthesize hemoglobin. Despite these facts, the available literature lacks consensus on the effects of altered EPO and iron levels on the different cell stages. Nevertheless, two facts seem to be unquestioned: first, a raised EPO concentration shortens marrow transit time, and, second, iron concentration affects erythropoiesis. If iron levels are too low to sufficiently supply the cells developing in the bone marrow, erythropoiesis is impaired. Because the underlying mechanisms are not entirely clear, we have decided to include these effects into the model by allowing the maturation velocity of reticulocytes to vary with plasma EPO concentration, but not the maturation velocity for erythroblasts. Consequently, the transit time for precursor cells in our model is between 6 and 8 days, the variability being mediated by the reticulocyte population. Furthermore, cells which are not able to synthesize a certain minimum amount of hemoglobin are assumed to get phagocytosed, i.e., a low iron concentration leads to a higher mortality rate of precursor cells. We assume that this is effected in the reticulocyte population class and have coded this into the model by allowing the mortality rate for reticulocytes to depend on plasma iron concentration. Since, for the current model, we are assuming sufficient iron supply, we can simplify the model by using a constant apoptosis rate for marrow reticulocytes. We choose a non-zero apoptosis rate to accommodate the fact that a mild degree of ineffective erythropoiesis is present even under iron replete conditions (Barosi et al. 1985; Stefanelli et al. 1984), and that it amounts to approximately 4–12 % of the total erythropoiesis (Lichtman et al. 2005).

Let $\mu^r \to r(t, \mu^r)$ denote the population density for the erythroblast population at time t with μ^r being the maturity of an erythroblast. The model equations are:

$$\begin{aligned} \frac{\partial}{\partial t} r(t, \mu^r) + \frac{\partial}{\partial \mu^r} r(t, \mu^r) &= \beta^r r(t, \mu^r), \\ r(t, \mu^r_{\min}) &= q(t, \mu^q_{\max}), \\ r(0, \mu^r) &= r_0(\mu^r), \end{aligned} \tag{5}$$

where β^r is a constant proliferation rate (Assumption 11), $r(t, \mu^r_{\min}) = q(t, \mu^q_{\max})$ describes the rate at which cells leave the CFU-E stage and enter the erythroblast cell stage (note that, according to Assumption 12, maturity coincides with age), $r_0(\mu^r)$ is the population density at $t = 0$, $13 = \mu^r_{min} \le \mu^r \le \mu^r_{max} = 18$ (Assumption 9) and $t \ge 0$.

We denote by $s(t, \mu^s)$ and μ^s the population density of the bone marrow reticulocyte population and the maturity of a reticulocyte, respectively. Based on our assumptions, we get the following model equations for the marrow reticulocyte population:

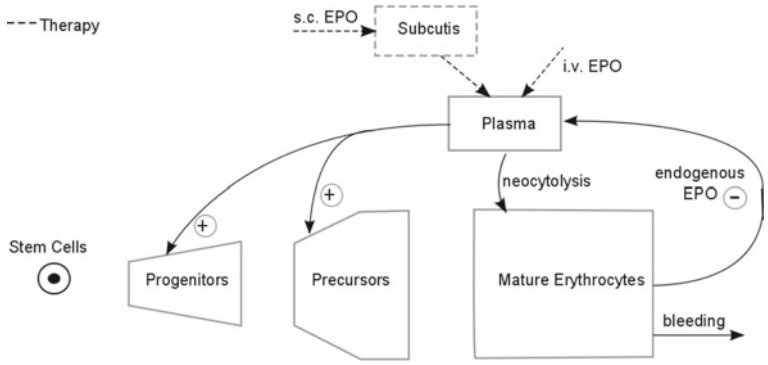

Fig. 2 Organizational diagram of the model

$$\begin{aligned} \frac{\partial}{\partial t}s(t,\mu^s) + v^s(E(t))\frac{\partial}{\partial \mu^s}s(t,\mu^s) &= -\alpha_0^s s(t,\mu^s), \\ v^s(E(t))s(t,\mu^s_{\min}) &= r(t,\mu^r_{\max}), \\ s(0,\mu^s) &= s_0(\mu^s), \end{aligned} \tag{6}$$

where $v^s(E(t))$ is the maturation velocity depending on EPO (Assumption 13), α_0^s denotes the rate of ineffective erythropoiesis (Assumption 15), $v^s(E(t))s(t,\mu^s_{\min}) = r(t,\mu^r_{\max})$ describes the rate at which cells leave the erythroblast cell stage and enter the reticulocyte cell stage, $r_0(\mu^s)$ is the population density at $t = 0, 18 = \mu^s_{\min} \leq \mu^s \leq \mu^s_{\max} = 21$ (Assumption 9) and $t \geq 0$. Note that the actual time that cells stay in this stage is between 1–3 days according to the maturation velocity. A slower maturation velocity causes the cells to reach "maximal maturity" later, whereas a faster maturation velocity shortens the transit time, i.e., the cells reach "maximal maturity" earlier.

Again we use a sigmoid function to describe the dependence of the maturation velocity v^s on the EPO concentration in plasma,

$$v^s(E(t)) = \frac{a_2 - b_2}{1 + e^{-k_2 E(t) + c_2}} + b_2, \tag{7}$$

where $E(t)$ is the EPO concentration in plasma at time t. Therefore, the maturation velocity increases with a rising concentration of EPO.

3.3 Erythrocytes and blood reticulocytes

Assumptions

16. The maximum age of erythrocytes in a healthy person is 120 days (which corresponds to the average erythrocyte lifespan in healthy adults).
17. Cells mature but do not proliferate.
18. The maturation rate of red blood cells is constant.

19. All erythrocytes carry the same amount of hemoglobin, and this stays constant during their life time.
20. There is a fixed rate of random daily breakdown of red blood cells (not to be confused with loss of erythrocytes due to senescence).
21. Neocytolysis is triggered when the plasma concentration of EPO is below a certain level.

Reticulocytes are released from the bone marrow into the blood stream, and within 1–2 days they mature to erythrocytes. Henceforth, when we discuss erythrocytes, we mean reticulocytes in blood and mature erythrocytes. Red blood cells are able to carry oxygen because of the contained hemoglobin that the cells synthesized during the precursor cell stage. In practice, not all cells have the same capacity to transport oxygen. For a healthy adult, however, the variance in hemoglobin content among erythrocytes is small. Therefore, Assumption 19 seems to be reasonable. A consequence of this assumption is that the oxygen carrying capacity of blood is directly proportional to the number of erythrocytes.

The circulating red blood cells have no nuclei and, therefore, they are not able to proliferate or to repair themselves. They are constantly suffering damage, and, after some time, they lose their flexibility and hence their ability to squeeze through small capillaries. In order to prevent damage to vessels, senescent cells are marked and phagocytosed by macrophages, primarily in the spleen. In a healthy adult, the life span of circulating red blood cells is about 120 days (see e.g., Jandl 1987), but it can markedly decrease in some pathologies. As we have explained in Sect. 2, a selective hemolysis of young erythrocytes can occur under certain circumstances (neocytolysis). In addition, a small number of cells die because of random daily breakdown, or are lost due to internal or external bleeding.

Denoting by $m(t, \mu^m)$ and μ^m the population density of erythrocytes and the age of erythrocytes we get the following model equations for the erythrocyte population:

$$\begin{aligned} \frac{\partial}{\partial t} m(t, \mu^m) + \frac{\partial}{\partial \mu^m} m(t, \mu^m) &= -\alpha^m(E(t), \mu^m) m(t, \mu^m), \\ m(t, 0) &= v^s(E(t)) s(t, \mu^s_{\max}), \\ m(0, \mu^m) &= m_0(\mu^m), \end{aligned} \tag{8}$$

where $m(t, 0) = v^s(E(t))s(t, \mu^s_{\max})$ describes the rate at which reticulocytes enter the blood stream, $m_0(\mu^m)$ is the population density at $t = 0$, $0 \le \mu^m \le \mu^m_{\max} = 120$ (Assumption 16) and $t \ge 0$. The mortality rate $\alpha^m(E(t), \mu^m)$ incorporates the effect of neocytolysis and the random daily breakdown (Assumptions 20 and 21). It is given by

$$\alpha^m(E(t), \mu^m) = \begin{cases} \alpha^m_r + \min\left(\dfrac{c_E}{E(t)^{k_E}}, b_E\right) & \text{for } E(t) < \tau_E,\ \mu^m_{n,\min} \le \mu^m \le \mu^m_{n,\max}, \\ \alpha^m_r & \text{otherwise,} \end{cases} \tag{9}$$

where α_r^m is the random daily breakdown, b_E, c_E, k_E are constants, τ_E is the threshold for $E(t)$ beneath which neocytolysis is triggered, and $[\mu_{n,\min}^m, \mu_{n,\max}^m]$ is the age-interval where neocytolysis is possible. For the simulations shown in this paper, we choose $\mu_{n,\min}^m = 14$ days and $\mu_{n,\max}^m = 21$ days.

3.4 Feedback via erythropoietin

Assumptions

22. Release of EPO is controlled by a negative feedback mechanism in response to the partial pressure of oxygen in blood.
23. Partial pressure of oxygen in blood is directly proportional to the number of erythrocytes (see also Assumption 19 in Sect. 3.3).
24. The degradation rate of EPO is constant.
25. The time delay between change in oxygen partial pressure/number of erythrocytes and adaptation of EPO production rate is negligible compared to the duration of development of erythrocytes.

The kidneys adjust the release of EPO according to the oxygen partial pressure in blood. If partial pressure of oxygen in blood is lower respectively larger than normal, then EPO production increases respectively decreases. Thus, the production of EPO is controlled by a negative feedback mechanism and allows for more red blood cells to be developed in case of deficient supply of the body with oxygen. However, this is not the only feedback function EPO performs. In addition, the body has the protective mechanism of neocytolysis in case of an excess of red blood cells. If EPO concentration drops below a certain threshold, macrophages start to phagocytose young erythrocytes (neocytes). This is an important mechanism to allow swift downward adaptation of RBC mass to changes in the environment, e.g., when high altitude dwellers descend to sea level (see Rice et al. 2001). See Eq. (9) in Sec. 3.3 for a model of neocytolysis.

A sigmoid function which depends on blood oxygen partial pressure is used to model the feedback involving the release of endogenous erythropoietin $E_{\text{in}}^{\text{end}}(t)$ from the kidneys into the plasma. As a consequence of Assumptions 22, 23 and 25 made above, the amount $E_{\text{in}}^{\text{end}}(t)$ of EPO released by the kidney per unit time can be directly computed by use of the total population of erythrocytes $M(t)$ (recall that this class consists of all circulating red blood cells):

$$E_{\text{in}}^{\text{end}}(t) = \frac{a_3 - b_3}{1 + e^{k_3 \tilde{M}(t) - c_3}} + b_3, \tag{10}$$

where $\tilde{M}(t) = 10^{-8} M(t)/TBV$ is a scaled erythrocyte "concentration" with $M(t) = \int_0^{\mu_{\max}^m} m(t, \mu^m)\, d\mu^m$ and TBV is the total blood volume. Thus, the release of EPO increases if the number of circulating red blood cells decreases. The dynamics of the endogenous EPO concentration $E^{\text{end}}(t)$ in plasma is described by the following ordinary differential equation:

$$\dot{E}^{\text{end}} = \frac{1}{TBV} E_{\text{in}}^{\text{end}}(t) - c_{\text{deg}}^{\text{end}} E^{\text{end}}(t), \tag{11}$$

where $E^{\text{end}}(t)$ is the endogenous EPO concentration in plasma, $E_{\text{in}}^{\text{end}}$ is the amount of EPO released by the kidneys per unit time and $c_{\text{deg}}^{\text{end}}$ describes the degradation rate of endogenous EPO (Assumption 24).

In the case of administration of rHuEPO, an additional ordinary differential equation is required to describe the change in the plasma concentration $E^{\text{ex}}(t)$ of the exogenous hormone,

$$\dot{E}^{\text{ex}}(t) = \frac{1}{TBV} E_{\text{in}}^{\text{ex}}(t) - c_{\text{deg}}^{\text{ex}} E^{\text{ex}}(t), \tag{12}$$

where $E_{\text{in}}^{\text{ex}}(t)$ is the rate at which the exogenous hormone is administered, $c_{\text{deg}}^{\text{ex}}$ is the rate at which the exogenous hormone is degraded. In the case of an intravenous administration, the total amount of the agent is injected into a vein within a very short time interval. In this case $E_{\text{in}}^{\text{ex}}(t)$ can be approximated by $E_0^{\text{ex}}(t)\delta_{t_0}(t)$, where E_0^{ex} is the amount of exogenous hormone administered and δ_{t_0} is the Dirac delta impulse located at t_0, the time when the administration takes place. The result is a sudden rise of the amount of the exogenous hormone in plasma, followed by a decay of the ESA level that depends on the degradation rate of the exogenous hormone, which varies for different ESAs. In contrast, in the case of a subcutaneous administration, the agent is injected under the skin and slowly diffuses from there into the plasma, which results in a continuous flow of agent into the plasma compartment and a slow rise in the plasma ESA level over a longer time than with intravenous administration. Subcutaneous administration, although biologically and economically more desirable, is relatively painful for the patient, and, therefore, intravenous administration is the more common administration method (Besarab et al. 2002). In addition, the degradation rate $c_{\text{deg}}^{\text{ex}}$ for exogenous EPO differs from the one for endogenous EPO and varies depending on the type of ESA. The overall concentration of EPO in plasma consists of the naturally produced erythropoietin and the administered rHuEPO

$$E(t) = E^{\text{ex}}(t) + E^{\text{end}}(t). \tag{13}$$

4 Numerics

For the simulations we chose a slight modification of an approximation scheme for age structured population model given in Kappel and Zhang (1993). The model equations are of type (1) which we write as

$$\frac{\partial}{\partial t}u(t,\mu) + \tilde{v}(t)\frac{\partial}{\partial \mu}u(t,\mu) = \kappa(t,\mu)u(t,\mu), \tag{14}$$

where we have set $\tilde{v}(t) = v(E(t))$ and $\kappa(t,\mu) = \big(\beta(E(t)) - \alpha(E(t), z(t), \mu)\big)$. The attribute μ which is used to distinguish between cells varies in $[\mu_{\min}, \mu_{\max}]$. We have the following initial and boundary conditions:

$$u(0,\mu) = \phi(\mu), \quad \mu_{\min} \le \mu \le \mu_{\max} \quad \text{and} \quad u(t,\mu_{\min}) = f(t), \quad t > 0. \tag{15}$$

Since Eq. (14) is linear, we have global existence of solutions on the strip $[0, \infty) \times [\mu_{\min}, \mu_{\max}]$ provided the functions f and κ are defined on $[0, \infty)$ respectively on $[0, \infty) \times [\mu_{\min}, \mu_{\max}]$ and are sufficiently smooth. The concept of solution is based on the method of characteristics, i.e., $u(t, \mu)$ is a solution of (14) and (15) if u is given by

$$
\begin{aligned}
u(t,\mu) &= \phi\left(\mu - \int_0^t \tilde{v}(\tau)\,d\tau\right) \exp\left(\int_0^t \kappa\Big(\tau, \mu - \int_\tau^t \tilde{v}(\rho)\,d\rho\Big)\,d\tau\right),\\
\mu &\geq \mu_{\min} + \int_0^t \tilde{v}(\tau)\,d\tau,\\
u(t,\mu) &= f(t - g(t,\mu)) \exp\left(\int_0^{g(t,\mu)} \kappa\left(t - g(t,\mu) + \tau, \mu_{\min} + \int_{t-g(\tau,\mu)}^{t-g(\tau,\mu)+\tau} \tilde{v}(\rho)\,d\rho\right) d\tau\right),\\
t &\geq g(t,\mu).
\end{aligned}
\tag{16}
$$

Here the function $\mu \to \tau = g(t, \mu)$ is the inverse of $\tau \to \mu = \mu_{\min} + \int_{t-\tau}^t \tilde{v}(\rho)\,d\rho$. Note that $\mu = \mu_{\min} + \int_0^t \tilde{v}(\tau)\,d\tau$ is equivalent to $t = g(t, \mu)$. If we have $\tilde{v}(t) \equiv 1$, which is the case for Eqs. (2), (3), (5), and (8), we get from (16)

$$
\begin{aligned}
u(t,\mu) &= \phi(\mu - t) \exp\left(\int_{\mu-t}^{\mu} \kappa(\tau + t - \mu, \tau)\,d\tau\right), \quad \mu - t \geq \mu_{\min},\\
u(t,\mu) &= f\big(t - (\mu - \mu_{\min})\big) \exp\left(\int_0^{\mu-\mu_{\min}} \kappa\big(\tau + t - (\mu - \mu_{\min}), \mu_{\min} + \tau\big)\,d\tau\right),\\
\mu - t &\leq \mu_{\min}.
\end{aligned}
\tag{17}
$$

Note that in this case the attribute μ is just the age of a cell.

For explaining the approximation scheme we first restrict ourselves to the case $\tilde{v}(t) \equiv 1, t \geq 0$, and $\kappa = \kappa(\mu)$, $\mu_{\min} \leq \mu_{\max}$. Then the representation (17) reduces to

$$
u(t,\mu) = \begin{cases} \phi(\mu - t) \exp\left(\int_{\mu-t}^{\mu} \kappa(\tau)\,d\tau\right) & \text{for } t \geq \mu - \mu_{\min},\\ f\big(t - (\mu - \mu_{\min})\big) \exp\left(\int_0^{\mu-\mu_{\min}} \kappa(\mu_{\min} + \tau)\,d\tau\right) & \text{for } t \leq \mu - \mu_{\min}. \end{cases}
\tag{18}
$$

We indicate the initial value ϕ by writing $u(t, \mu) = u(t, \mu; \phi)$.

4.1 Formulation as an abstract Cauchy problem

We assume that $\phi \in L^2 := L^2(\mu_{\min}, \mu_{\max})$ and define the operators $S(t) : L^2 \to L^2$ by

$$S(t)\phi = u(t, \cdot; \phi), \quad t \geq 0, \ \phi \in L^2. \tag{19}$$

Using the representation (18) it can be shown that—in case $f \equiv 0$ – $S(t)$, $t \geq 0$, is a C_0-semigroup on L^2 (see Kappel and Zhang 1993, for results on C_0-semigroups, evolution operators and approximation see also Ito and Kappel 2002). The infinitesimal generator $\mathscr{A}$ of this semigroup is given by ($' = d/d\mu$)

$$\begin{aligned} \operatorname{dom} \mathscr{A} = \big\{ & \phi \in L^2 \big| \phi \text{ is absolutely continuous on } [\mu_{\min}, \mu_{\max}], \\ & \phi(\mu_{\min}) = 0, \ \phi' - \kappa\phi \in L^2 \big\}, \\ \mathscr{A}\phi = & -\phi' + \kappa\phi, \quad \phi \in \operatorname{dom} \mathscr{A}. \end{aligned} \tag{20}$$

For $\phi \in L^2$ respectively $\phi \in \operatorname{dom} \mathscr{A}$, $y(t) = S(t)\phi$ is a mild solution respectively a strong solution of the abstract Cauchy problem

$$\dot{y}(t) = \mathscr{A} y(t), \quad y(0) = \phi \in L^2. \tag{21}$$

For $f \not\equiv 0$ we define the functions $f_n(t, \mu) = f(t)\delta_n(\mu), t \geq 0, \mu_{\min} \leq \mu \leq \mu_{\max}, n = 1, 2, \ldots$, with

$$\delta_n(\mu) = \begin{cases} -2n^2(\mu - \mu_{\min} - 1/n) & \text{for } \mu_{\min} \leq \mu \leq \mu_{\min} + 1/n, \\ 0 & \text{otherwise,} \end{cases}$$

i.e., $(\delta_n)_{n=1,2,\ldots}$ is a sequence of functions approximating the δ-distribution. Let $y_n(\cdot), n = 1, 2, \ldots$, be a mild solution of the nonhomogeneous Cauchy problem

$$\dot{y}(t) = \mathscr{A} y(t) + f_n(t, \cdot), \quad y(0) = \phi \in L^2, \tag{22}$$

which can be represented as

$$y_n(t) = S(t)\phi + \int_0^t S(t - s) f_n(s, \cdot)\, ds, \quad t \geq 0.$$

Then it can be shown that $\lim_{n\to\infty} y_n(t)(\cdot) = u(t, \cdot)$ in $L^2, t \geq 0, \mu_{\min} \leq \mu \leq \mu_{\max}$, where $u(t, \mu)$ is given by (18).

Since the range for the attribute is different for the cells populations considered, it is useful to normalize these attributes such that the range of the normalized attribute ξ is [0, 1]. In order to achieve this we define the mapping

$$h(\xi) = \mu_{\min} + (\mu_{\max} - \mu_{\min})\xi, \quad 0 \leq \xi \leq 1,$$

with its inverse

$$H(\mu) = h^{-1}(\mu) = \frac{\mu - \mu_{\min}}{\mu_{\max} - \mu_{\min}}, \quad \mu_{\min} \le \mu \le \mu_{\max}.$$

We set $w = \mu_{\max} - \mu_{\min}$ and define on $L^2(0,1)$ the norm $\|\tilde{\phi}\|_w = w^{1/2}\|\tilde{\phi}\|_{L^2(0,1)}$. The space $L^2(0,1)$ endowed with the norm $\|\cdot\|_w$ will be denoted by L^2_w. The spaces L^2 and L^2_w are isomorphic with the isomorphism $\Xi : L^2 \to L^2_w$ and its inverse given by

$$\Xi\phi = \phi \circ h, \quad \phi \in L^2, \quad \text{and} \quad \Xi^{-1}\tilde{\phi} = \tilde{\phi} \circ H, \quad \tilde{\phi} \in L^2_w.$$

On the space L^2_w we get the C_0-semigroup $\tilde{S}(t) = \Xi S(t)\Xi^{-1}$, $t \ge 0$, with infinitesimal generator

$$\begin{aligned} \operatorname{dom} \tilde{\mathscr{A}} &= \Xi(\operatorname{dom} \mathscr{A}), \\ \tilde{\mathscr{A}} &= \Xi \mathscr{A} \Xi^{-1}. \end{aligned} \tag{23}$$

The Cauchy problem (22) is transformed to

$$\dot{\tilde{y}}(t) = \tilde{\mathscr{A}}\tilde{y}(t) + f(t)\tilde{\delta}_n, \quad \tilde{y}(0) = \Xi\phi = \phi \circ h, \quad t \ge 0, \ n = 1, 2, \ldots, \tag{24}$$

with

$$\tilde{\delta}_n(\xi) = (\Xi\delta_n)(\xi) = \begin{cases} -2n^2(w\xi - 1/n) & \text{for } 0 \le w\xi \le 1/n, \\ 0 & \text{otherwise.} \end{cases}$$

In the general case of Eqs. (14), (15) we get, instead of (22), a linear evolution equation of the form

$$\dot{y}(t) = \mathscr{A}(t)y(t) + f_n(t, \cdot), \quad y(0) = \phi \in L^2,$$

with

$$\begin{aligned} \operatorname{dom} \mathscr{A}(t) = \big\{ \phi \in L^2 \big| \, & \phi \text{ is absolutely continuous on } [\mu_{\min}, \mu_{\max}], \\ & \phi(\mu_{\min}) = 0, \ \tilde{v}(t)\phi' - \kappa(t, \cdot)\phi \in L^2 \big\}, \\ \mathscr{A}(t)\phi = -\tilde{v}(t)\phi' + \kappa(t, \cdot)\phi, \quad & \phi \in \operatorname{dom} \mathscr{A}(t). \end{aligned}$$

The Cauchy problem corresponding to (24) is

$$\dot{\tilde{y}}(t) = \tilde{\mathscr{A}}(t)\tilde{y}(t) + f(t)\tilde{\delta}_n, \quad \tilde{y}(0) = \Xi\phi = \phi \circ h, \quad t \ge 0,$$

with

$$\begin{aligned}\operatorname{dom}\tilde{\mathscr{A}}(t) = \big\{\tilde{\phi} \in L^2_w \,\big|\, &\tilde{\phi} \text{ is absolutely continuous on } [0,1],\\ &\tilde{\phi}(0) = 0,\ \tilde{v}(t)\tilde{\phi}' - \kappa(t,h(\cdot))\tilde{\phi} \in L^2_w\big\},\\ \tilde{\mathscr{A}}(t)\tilde{\phi} = -\tilde{v}(t)\tilde{\phi}' + \kappa(t,h(\cdot))\tilde{\phi},&\quad \tilde{\phi} \in \operatorname{dom}\tilde{\mathscr{A}}(t).\end{aligned}$$

4.2 Approximation

In order to get an approximation scheme for the solutions of (24) we define, following the approach in Kappel and Zhang (1993), a sequence of basis elements in L^2_w by

$$e_j(\xi) = w^{-1/2}L_j(-1+2\xi), \quad 0 \le \xi \le 1,\ j = 0,1,\dots, \tag{25}$$

where L_j is the jth Legendre polynomial. It is easy to see that the sequence e_j, $j = 0,1,\dots$, is an orthogonal sequence in L^2_w with $\langle e_j, e_k\rangle_{L^2_w} = 0$ for $j \ne k$ and $= (2j+1)^{-1}$ for $j = k$. We define the subspaces $X^N \subset L^2_w$ by

$$X^N = \operatorname{span}(e_0,\dots,e_N), \quad N = 0,1,\dots\ .$$

Let P^N be the orthogonal projection $L^2_w \to X^N$. Following Kappel and Zhang (1993) we define the approximating generators $\tilde{\mathscr{A}}^N$ on X^N by

$$\tilde{\mathscr{A}}^N\tilde{\phi} = -w^{-1}\tilde{\phi}' + P^N((\kappa\circ h)\tilde{\phi}) - \delta^N\tilde{\phi}(0), \quad \tilde{\phi} \in X^N,\ N = 0,1,\dots\ . \tag{26}$$

Here δ^N is the approximating delta impulse on X^N, i.e., $\delta^N \in X^N$ is defined by

$$\langle \delta^N, \tilde{\phi}\rangle_{L^2_w} = \tilde{\phi}(0), \quad \tilde{\phi} \in X^N.$$

The last term on the right-hand side of (26) accounts for the fact that $\tilde{\phi} \in X^N$ in general is not in dom $\tilde{\mathscr{A}}$. Concerning the first term on the right-hand side of (26) we should observe that $\tilde{\phi}' \in X^N$ for $\tilde{\phi} \in X^N$.

The solution segments $y(t) = u(t,\cdot)$ of the solution given by (18) are given as the limit $\lim_{n\to\infty} y_n(t)$ in L^2, where $y_n, n = 1,2,\dots$, is the mild solution of the Cauchy problem (22). The function $\tilde{y}(t) = \Xi y(t)$ solves (24). The approximations $\tilde{y}^N(t)$, $N = 0,1,\dots$, for $\tilde{y}(t)$ are obtained as the solutions of the following Cauchy problems in the finite dimensional subspaces X^N:

$$\frac{d}{dt}\tilde{y}^N(t) = \tilde{\mathscr{A}}^N\tilde{y}^N(t) + \delta^N f(t), \quad \tilde{y}^N(0) = P^N\Xi\phi. \tag{27}$$

The approximations $u^N(t,\mu)$ for $u(t,\mu)$ are given by

$$u^N(t,\mu) = \Xi^{-1}\big(\tilde{y}^N(t)\big)(\mu) = \tilde{y}^N(t)\left(\frac{\mu-\mu_{\min}}{\mu_{\max}-\mu_{\min}}\right), \quad t \ge 0,\ \mu_{\min} \le \mu \le \mu_{\max}.$$

We have $\lim_{N\to\infty} u^N(t,\cdot) = u(t,\cdot)$ in L^2 uniformly for t in bounded intervals (compare Kappel and Zhang 1993 [Theorem 4.3] for the case $f \equiv 0$).

In the case of Eqs. (14), (15) the approximating operators $\tilde{\mathscr{A}}^N(t)$ are given by

$$\tilde{\mathscr{A}}^N(t)\tilde{\phi} = -w^{-1}\tilde{\phi}' + P^N(\kappa(t,h(\cdot))\tilde{\phi}) - \delta^N\tilde{\phi}(0), \quad \tilde{\phi} \in X^N,\ N = 0,1,\dots,$$

and the approximations for $u(t,\mu)$ are $u^N(t,\mu) = \Xi^{-1}(\tilde{y}^N(t))$, $N = 0,1,\dots,$ where $\tilde{y}^N$ solves

$$\frac{d}{dt}\tilde{y}^N(t) = \tilde{\mathscr{A}}^N(t)\tilde{y}^N(t) + \delta^N f(t), \quad \tilde{y}^N(0) = P^N\Xi\phi.$$

Finally one has to compute matrix representations of the operators $\tilde{\mathscr{A}}^N$ respectively of $\tilde{\mathscr{A}}^N(t)$ and coordinate vectors of the approximating delta-impulses δ^N and of the projections $P^N\Xi\phi$. We refer to Kappel and Zhang (1993) for these straightforward, but lengthy computations.

5 Simulation results

5.1 General remarks

The model presented in Sect. 3 consists of five partial differential equations [Eqs. (2), (3), (5), (6), and (8)], two ordinary differential equations [Eqs. (11) and (12)], and the auxiliary equations [Eqs. (4), (7), (9), (10), and (13)]. Altogether we have 30 parameters in the model to which values have to be assigned. For a list of all parameters, as well as their values and units, see Table 2.

Values taken from the literature were used to make a first educated guess on the parameters of the model, including also a table with the sizes of the erythroid pools in Lichtman et al. (2005, Chap. 30). In this book, the numbers for different erythroid cell types per kg body weight are given for healthy adults. From this information, the cell population sizes for a 75-kg adult male were calculated (see Table 1). These results were used to estimate the model parameters for the steady state. Plots of the model output are presented in Fig. 3. Note that each cell population was started with 1×10^8 cells. Therefore, it requires some time for the model output to reach equilibrium. Moreover, the constants for the feedback law and the auxiliary equations were

Table 1 Total numbers of cells for different cell types in healthy adults (see Lichtman et al. 2005, Chap. 30)

Cell type	Observed ($\times 10^8$ per kg)	75 kg
Proerythroblasts	1	75×10^8
Erythroblasts	49	36.75×10^{10}
Marrow reticulocytes	82	61.5×10^{10}
Red blood cells (incl. blood retic.)	3,331	24.98×10^{12}

Table 2 Model parameters, values and units

Parameter	Meaning	Value	Unit
β^p	Proliferation rate for BFU-E cells	0.2	1/day
β^q	Proliferation rate for CFU-E cells	0.57	1/day
β^r	Proliferation rate for erythroblasts	1.024	1/day
$\mu^p_{\max}$	Maximal maturity for BFU-E cells	7	Days
$\mu^q_{\min}$	Minimal maturity for CFU-E cells	7	Days
$\mu^q_{\max}$	Maximal maturity for CFU-E cells	13	Days
$\mu^r_{\min}$	Minimal maturity for erythroblasts	13	Days
$\mu^r_{\max}$	Maximal maturity for erythroblasts	18	Days
$\mu^s_{\min}$	Minimal maturity for marrow reticulocytes	18	Days
$\mu^s_{\max}$	Maximal maturity for marrow reticulocytes	21	Days
α^s_0	Rate of ineffective erythropoiesis	0.089	1/day
α^m_r	Intrinsic mortality rate for erythrocytes	0.005	1/day
a_1, b_1	Constants for the sigmoid apoptosis rate for CFU-E cells	0.35, 0.07	1/day
c_1, k_1	Constants for the sigmoid apoptosis rate for CFU-E cells	3, 0.14	Dimensionless, ml/mU
a_2, b_2	Constants for the sigmoid maturation velocity for marrow reticulocytes	2, 0.35	Dimensionless
c_2, k_2	Constants for the sigmoid maturation velocity for marrow reticulocytes	2.3, 0.2	Dimensionless, ml/mU
a_3, b_3	Constants for the sigmoid function governing the release of EPO from the kidneys	9,000, 10,000	mU/day
c_3, k_3	Constants for the sigmoid function governing the release of EPO from the kidneys	9.1, 0.2	Dimensionless, ml
$\mu^m_{n,\min}$	Lower bound of erythrocytes which are possibly exposed to neocytolysis	14	Days
$\mu^m_{n,\max}$	Lower bound of erythrocytes which are possibly exposed to neocytolysis	21	Days
$\mu_{\max}$	Maximal life span for erythrocytes	120	Days
b_E	Constant in the mortality rate for erythrocytes	0.1	1/day
c_E	Constant in the mortality rate for erythrocytes	3.5	$\mathrm{mU}^3/\mathrm{ml}^2$
k_E	Exponent in the mortality rate for erythrocytes	3	$\mathrm{mU}^3/\mathrm{ml}^2$
τ_E	EPO threshold for neocytolysis	9.8	mU/ml
$c^{\mathrm{end}}_{\mathrm{deg}}$	Degradation rate of EPO released by the kidney	25/24	1/day
$c^{\mathrm{ex}}_{\mathrm{deg}}$	Degradation rate of administered EPO (Epoetin-α)	8.5/24	1/day
S_0	Rate at which cells are committing to the erythroid lineage	10^8	1/day
TBV	Total blood volume	5,000	ml

chosen such that solutions stay near the desired equilibrium, when started near the steady state, and that the solutions always tend to the steady state (compare Fig. 3). In addition, we also used the fact that in a healthy adult the production rate of

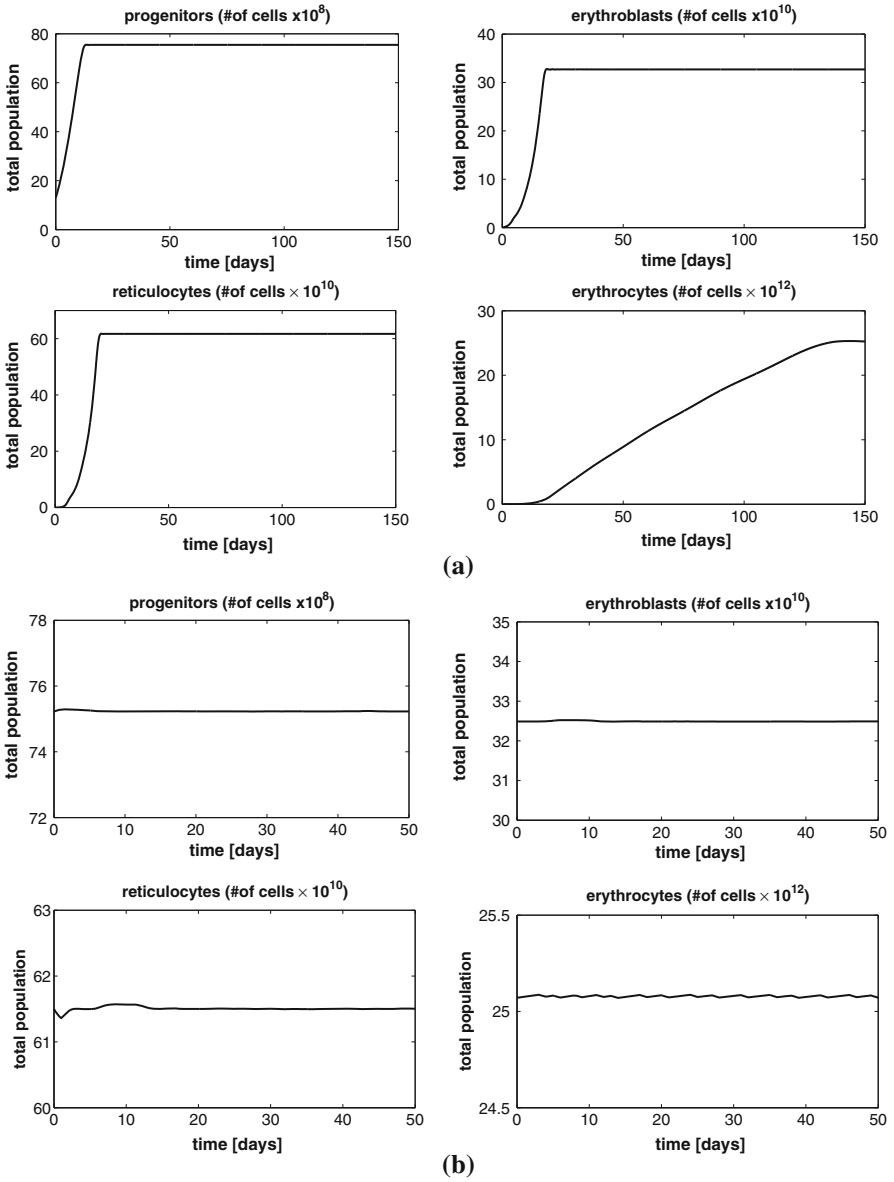

Fig. 3 Simulations for a fictitious 75 kg male starting with 1×10^8 cells (**a**) and starting near the equilibrium with the feedback control switched on (**b**)

erythrocytes can increase about threefold and that, by providing drugs (ESAs and iron), this rate can be increased to about fivefold (Goodnough 2002; Finch 1982). The simulations presented in the following subsections were done using parameter values obtained by the procedures described above. *It is emphasized that for all simulations the same set of parameters has been used. Parameters have not been adapted for*

a specific simulation in order to improve data fitting. Furthermore, it should be noted that no parameter identification was done but that parameter values were assigned using what one could call an "educated guess". The satisfying behavior of the model reflects the efforts during model development to adequately take into consideration the underlying physiological mechanisms.

5.2 High altitude dwellers

A low number of erythrocytes as well as an inappropriately high number is detrimental for the body. The feedback through erythropoietin acting on the progenitor and precursor cells is reasonably fast in case of a decreased number of red blood cells, but it is very slow when red cell mass exceeds normal values. This effect is due to the relatively long life span of erythrocytes of about 120 days. Thus, even if the production of precursor cells is distinctly reduced, the effect on the number of erythrocytes circulating in the blood is only a small one in the short run. This suggests that an additional mechanism is needed which acts faster in the case of RBC mass exceeding normal values. Indeed, as we already discussed in Sect. 2, physiologists discovered this mechanism, neocytolysis, not too long ago. The essential feature of neocytolysis is that active hemolysis of young red blood cells is triggered when the concentration of EPO in plasma drops below a certain threshold, which would be the case if the partial pressure of oxygen in blood were high because of an abundance of RBCs. Neocytolysis is probably responsible for the anemia of astronauts returning from space missions (Alfrey et al. 1996; Udden et al. 1995), can be observed in high altitude dwellers descending to sea level (Rice et al. 2001), and seems to contribute to the erythrocyte degradation in patients treated with ESAs (Alfrey and Fishbane 2007; Chang et al. 2009; Rice et al. 1999). For a summary of several studies concerning neocytolysis in descending high altitude dwellers and astronauts returning from space mission, see Rice and Alfrey (2005). The observed effect on RBC mass seems to be similar throughout the studies. In the first few days (7–10 days) RBC mass reduces by 9–18 %. If further adaption is necessary, RBC mass reduction progresses more slowly and seems to be mediated mainly through reduced erythropoiesis.

Figure 4 shows the simulation results for a 75 kg man descending from high altitude to sea level assuming an increased number of mature erythrocytes, 40 % above normal levels. We present the development of the RBC mass during the first 5 weeks (35 days) considering neocytolysis (solid line) and neglecting it (dashed line). Several interesting observations can be made: first, the predicted reduction of the RBC mass is within a physiologically meaningful range. The total number of RBC has decreased by $\sim$11.3 % after 7 days and by $\sim$ 14.5 % after 10 days (see Fig. 4). Secondly, it has been suggested that neocytolysis is only a prominent factor in the first few days (see Rice and Alfrey 2005). In the simulation, the influence of the destruction of young erythrocytes plays a key role in the first 10 days but becomes almost negligible in comparison to the influence of a reduced erythropoiesis later on. This can be seen from the fact that between days 0 and 10, the slopes of the solid and the dashed lines differ distinctly, whereas they become very similar later on (see Fig. 4).

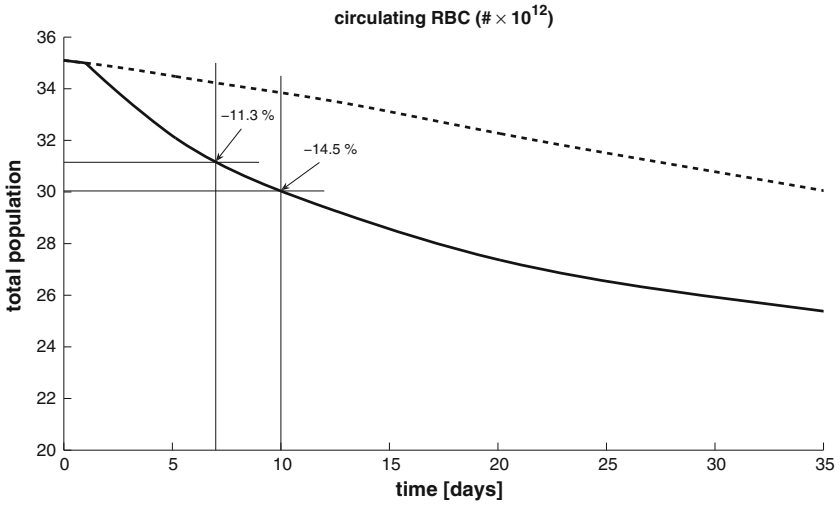

Fig. 4 Modeled changes in the number of circulating RBCs in a high altitude dweller descending to a lower altitude: model output with (*solid line*) and without (*dashed line*) neocytolysis during days 0–35

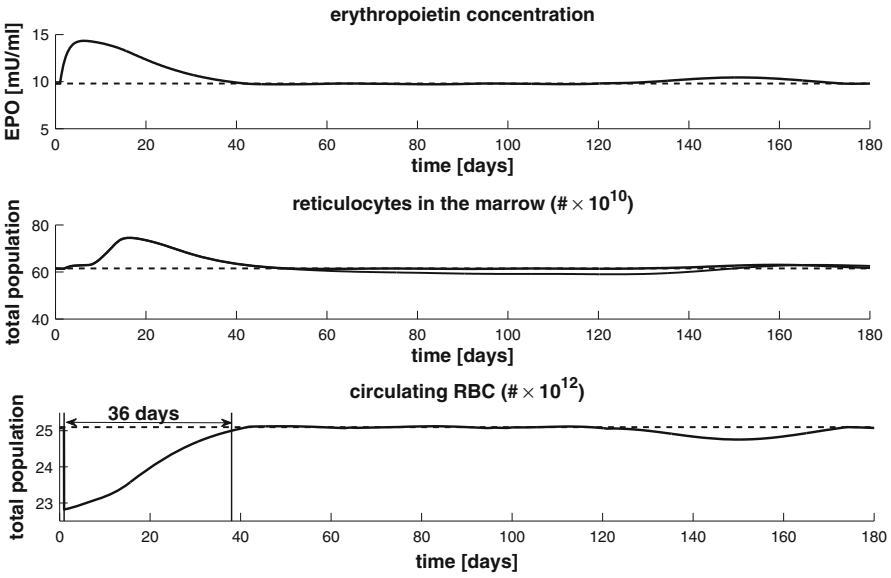

Fig. 5 Simulation of donation of 550 ml blood. The mean recovery period according to Pottgiesser et al. (2008) is 36 days (indicated in the *bottom graph* by a *vertical line*)

5.3 Blood donation

Figures 5 and 6 show simulations of a standard blood donation of 550 ml obtained from a person weighing 75 kg. The simulation starts in the steady state, and after one day,

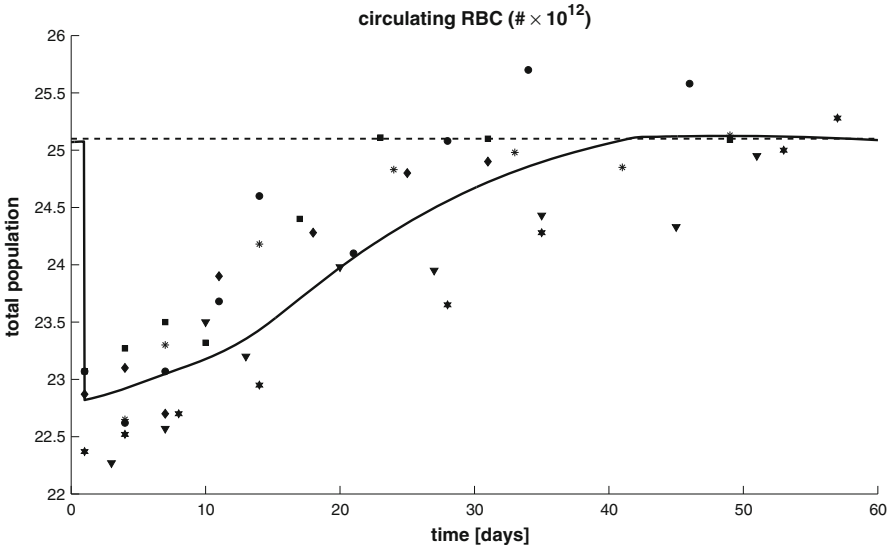

Fig. 6 Simulation of donation of 550 ml blood. Data points taken from Pottgiesser et al. (2008). *Different symbols* refer to different patients

9 % of the erythrocyte population is lost due to blood donation. Figure 5 illustrates how erythropoiesis adapts to this stress situation and drives the system back to the original state. Directly after blood donation, the model reacts to the decreased oxygen carrying capacity by releasing more EPO into the plasma compartment (see the top graph in Fig. 5). A small increase in the number of reticulocytes can be observed almost immediately. Their number increases slightly due to a reduction in marrow transit time, which is visible in the middle graph of Fig. 5 as a small initial upward shift. The dominant effect can be seen within a few days when, because of better surviving probabilities of the progenitor cells (due to the increased erythropoietin concentration), more cells enter the precursor cell class and, as a consequence, more reticulocytes mature. The population of circulating erythrocytes increases, as shown in the bottom graph of Fig. 5, and reaches its initial value within less than 40 days after blood donation.

These results coincide with the findings in a study by Pottgiesser et al. (2008). In this study, the recovery of total hemoglobin (tHb) after a standard blood donation in 29 healthy male volunteers (mean ± standard deviation: 76.6 ± 11.2 kg, 30 ± 10 years, 181 ± 7 cm) was investigated: "After donation of approximately 550 ml of whole blood, the lost amount of tHb of 75 ± 15 g (8.8 ± 1.9 % tHb baseline) was recovered after a mean of 36 ± 11 days (range: 20–59 days). … In many subjects a delay of approximately 5 days was observed after blood donation in which no or only a minor increase in tHb occurred. After this short delay, a continuous restoration of tHb was noted …"[1]. The average recovery time of 36 days is plotted as a vertical line in Fig. 5.

[1] Quoted from Pottgiesser et al. (2008).

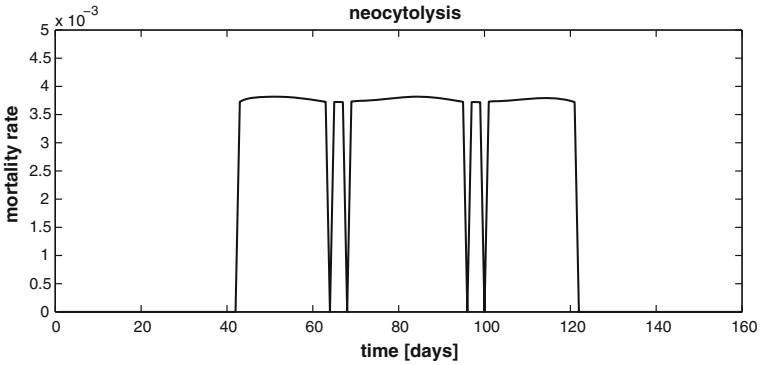

Fig. 7 Neocytolysis (corresponding to the simulation depicted in Fig. 5)

It is generally agreed that iron stores decrease after blood donation. In Pottgiesser et al. (2008), first-time, infrequent and frequent donors were included in the study. In some test subjects, a slight iron deficiency could be an explanation for a prolonged recovery period. Fowler and Barner (1942) found that the mean recovery period in young men who donated blood repeatedly could be shortened from 49 to 35 days by administration of supplementary iron.

In addition to this general information, there were also 6 representative sets of data of test subjects included in Pottgiesser et al. (2008). The data were given in percentages of the individual tHb at baseline (=100 %) at the beginning of the trial, i.e., before blood donation. The steady state of the simulations presented here were defined to be the RBC mass baseline, and we plotted the relative changes according to the data in Pottgiesser et al. (2008) together with the model predictions (see Fig. 6). Although a comparison of the model simulation and the study can only be done with some reservations—tHb is not necessarily always directly proportional to the number of erythrocytes—the results indicate that the model can simulate quite accurately the physiologic response to a typical blood donation in an average healthy male. The predicted recovery period agrees with the mean recovery time in Pottgiesser et al. (2008) and Fowler and Barner (1942) (after iron supplementation), and the individual data points correspond well with the simulation for an average adult.

Another fact that can be observed in the model—which is possibly more of theoretical importance—is that the system tends to overcompensate for the loss of RBC mass. This is because the effect of the negative feedback loop, which affects mainly the CFU-E cells, on the number of erythrocytes is relatively slow. It takes some time until progenitor cells mature to erythrocytes. Therefore, the cells entering the blood stream are cells that survived under a certain level of EPO days ago. Consequently, more cells than normal enter the blood stream during a period of a few days when the level of erythropoietin decreases to normal. Thus, neocytolysis is triggered in these simulations because of a small excess of RBC mass. See Fig. 7 for a plot showing the component of the mortality rate due to neocytolysis. Note that the mortality rate is very small throughout the simulation (<0.004), but continues over a considerable time (around days 40–120). Figure 5 shows that there is a slight drop in the number of erythrocytes around day 120 which continues for about 30 days. The system reacts to this

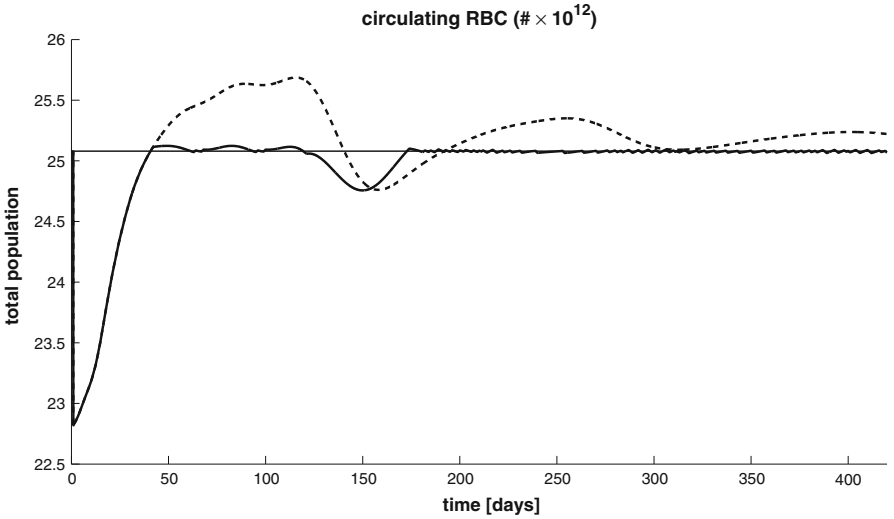

Fig. 8 Simulation over a long time interval after blood donation, model output with neocytolysis (*solid line*) and without neocytolysis (*dashed line*)

drop and slightly increases erythropoiesis. The reason for the drop in the erythrocyte population after around day 120 is the following: after the blood loss, the model predicts a considerable elevation of progenitor and precursor cells. Thus, the number of cells entering blood circulation at a certain time $\hat{t}$ is higher than usual. At the moment, one of the model assumptions is that erythrocytes die exactly at the age of 120 days. Therefore, at time $\hat{t} + 120$ all the cells that entered the erythrocyte class at time $\hat{t}$ die at once. This means that, because the production rate of cells between days 1 and 50 was higher in the simulation, more cells reach the maximum age at days 121–170 and die, causing the erythrocyte population to drop. Continuing the simulation for 200 additional days shows that this drop remains the only one, and that the system does not show oscillatory behavior around the steady state. Simulations without neocytolysis show more pronounced fluctuations and small oscillations around the steady state. See Fig. 8 for a simulation run over a long time interval (more than 400 days) after blood donation comparing model output with and without neocytolysis.

5.4 Pre-surgical administration of erythropoiesis stimulating agents

Simulation results considering administration of ESAs in healthy adults are presented in this subsection. For instance, it is common practice to treat patients that have to undergo elective surgeries with rHuEPO in advance. This is done in order to increase the hemoglobin in these subjects with the objective that the need for allogenic blood transfusion after the surgery is reduced and/or the patients are able to donate blood preoperatively for allogeneic blood transfusion. However, acquisition costs of erythropoiesis stimulating agents are high and it is in the health care systems interest to choose a most cost-effective administration scheme (Jaspan 2007).

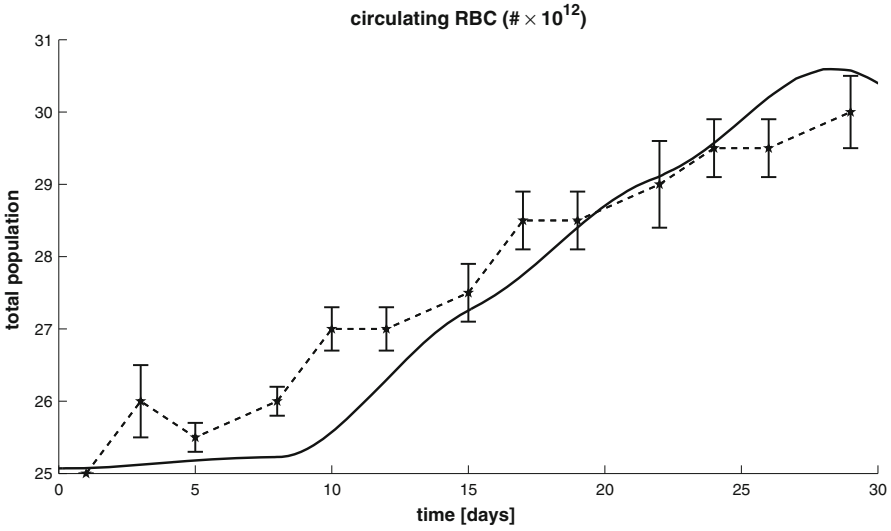

Fig. 9 Administration of Epoetin-α in a healthy adult. Data points are taken from Cheung et al. (2001) and the measured data (± 2 standard error means) are connected with *straight dashed lines*. Model simulations (*solid line*) for this administration scheme ($4 \times 40{,}000$ U once a week) are also added to the graph

When treating healthy persons with ESAs the common administration route is subcutaneous (s.c.) administration. Data concerning pharmacokinetics and pharmacodynamics of Epoetin-α for a drug administration of 40,000 U once weekly (q.w.) s.c. for 4 weeks in healthy persons are available in Cheung et al. (2001). The evaluated pharmacokinetic profile of Epoetin-α was the following: mean peak in serum erythropoietin concentrations was 861 ± 445.1 mU/ml after 16.1 ± 4.27 h after administration with a mean half-life value of 15.0 ± 6.12 h. As one can see there is a huge variability in the pharmacokinetic profile of this ESA. We used the mean values (a peak in serum EPO levels of 861 mU/ml and a half-life of 15 h) and the described administration scheme of 40,000 U q.w. s.c. for 4 weeks to run model simulations and compared it to the pharmacodynamic data of the study (see Fig. 9). The model predicts the average and terminal qualitative behavior of the test subjects to the drug administration well and also quantitatively the results are quite satisfactory. During the first 12 days of treatment the simulations underestimate the red cell mass, but afterwards the simulations fit the data adequately. The delayed reaction of the system in the beginning could eventually be explained by an underestimated ability of the body to release reticulocytes when exposed to supraphysiologic levels of EPO.

Concerning pre-surgical administration of ESAs, we compared the model output to the results of a study by Feagan et al. (2000). In this study patients undergoing primary hip joint arthroplasty were administered Epoetin-α starting 4 weeks prior to the surgery. 201 patients were assigned to 3 different groups: a low dose group—receiving 20,000 U Epoetin-α q.w. s.c., a high dose group—receiving 40,000 U Epoetin-α q.w. s.c., and a control group—receiving a placebo. All three groups were additionally treated with supplementary iron. Therefore, it is reasonable to assume that the RBC production rate of the test subjects was not impaired by a lack of iron. Thus, our basic

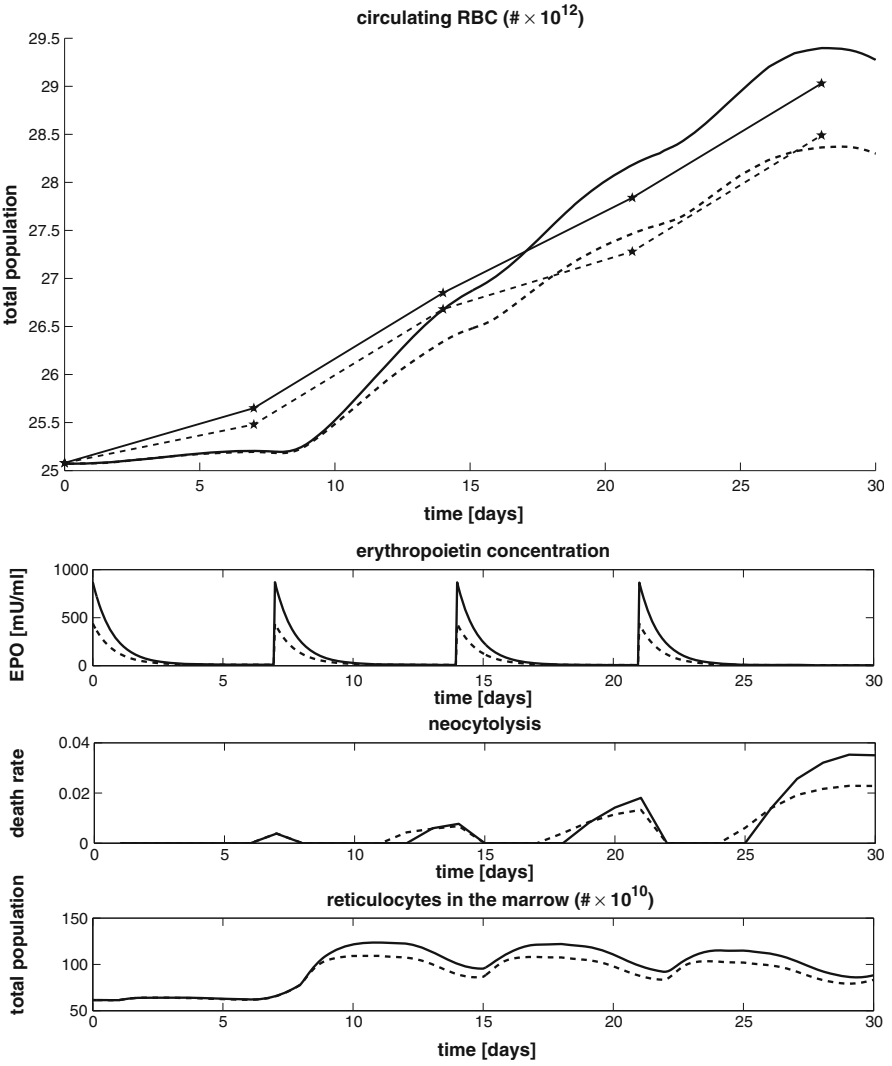

Fig. 10 Preoperative administration of Epoetin-α. Data points are taken from Feagan et al. (2000) and the measured data (*stars*) are connected by *straight lines*. Results of model simulations for this administration scheme are also added to the graph. *Dashed lines* are used for the low-dose group (4×20,000 U once a week) and *solid lines* for the high-dose group (4×40,000 U once a week), respectively

model assumption is valid and the simulations are comparable to the observed data. Because Feagan et al. (2000) did not publish any pharmacokinetic data we orientated ourselves on the study of Cheung et al. (2001) (note that both used the same drug and a similar administration scheme). The pharmacodynamic reaction in these two studies differed slightly, probably because the demographics of the test subjects are very different. For instance, a mean age of 28.1 ± 6.51 in Cheung et al. (2001) compared to a mean age of 68.9 ± 10.8 and 67.3 ± 11.0 in the low-dose and high-dose group, respectively, in Feagan et al. (2000); 53 % males in Cheung et al. (2001) compared

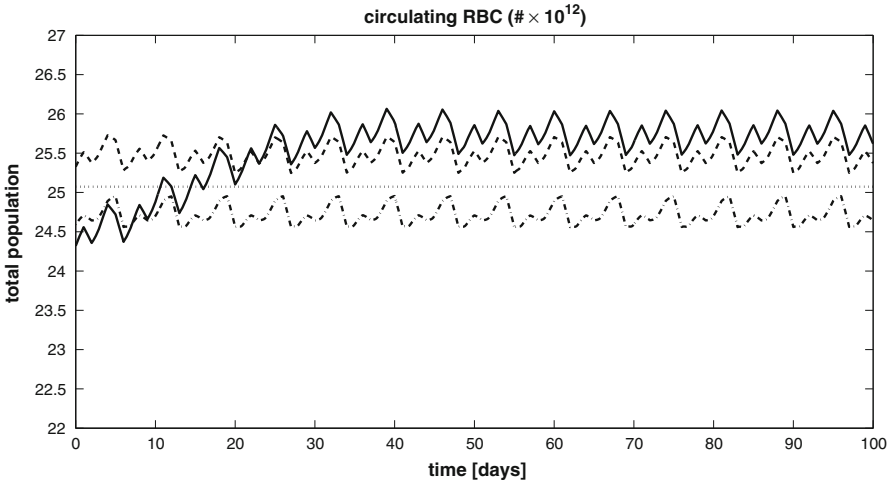

Fig. 11 Consequence of different life spans on the amount of ESA (here: Epoetin-α) which has to be administered. The *dotted line* represents the baseline for a healthy adult. Administration scheme: 2× per week; accumulated weekly dose and life span of RBCs: 8,000 U and 120 days (*solid line*), 9,500 U and 90 days (*dashed line*), 14,000 U and 60 days (*dash-dotted line*)

to 7.6 and 11.4 % males in the low-dose and high-dose group, respectively, in Feagan et al. (2000).

A setup similar to the one used by Feagan et al. (2000), considering the administration scheme, is used for the simulations. Additionally, the pharmacokinetic data from Cheung et al. (2001) are used, but the half-life of Epoetin-α was slightly reduced to 13 h, which lies well within the data's standard deviation. The pharmacodynamic data measured in Feagan et al. (2000) was the hemoglobin concentration of the test subjects. In order to incorporate the observations into the plots, a method similar to the method used in Sect. 5.3 with the data from Pottgiesser et al. (2008) was used herein. Again, the model predicts the average reaction of the test subjects to the drug administration quite well (see Fig. 10). At the beginning of the treatment simulations underestimate the red cell mass, but afterwards the simulations fit the data adequately. In Feagan et al. (2000) the authors stated that they were quite surprised that doubling the dose from 20,000 to 40,000 U lead only to a slight increase in hemoglobin concentration. Interestingly, our model predicts only a minor difference in the number of marrow reticulocytes between the low-dose and high-dose group. This possibly provides an explanation why the red cell masses in the two groups differ only slightly. Another observation is that neocytolysis gets more prominent in the intermediate phases from week to week. Because of a rising excess in red cell mass, endogenous erythropoietin gets more and more suppressed. The administered Epoetin-α gets almost completely decomposed within 4 days and therefore the EPO concentration in plasma drops beneath the threshold where the destruction of neocytes is triggered.

5.5 Comparison of administration regimens for ESAs

The simulations presented above, which modeled available literature data, showed very good agreement with the real-life data in all cases. This indicates that the model

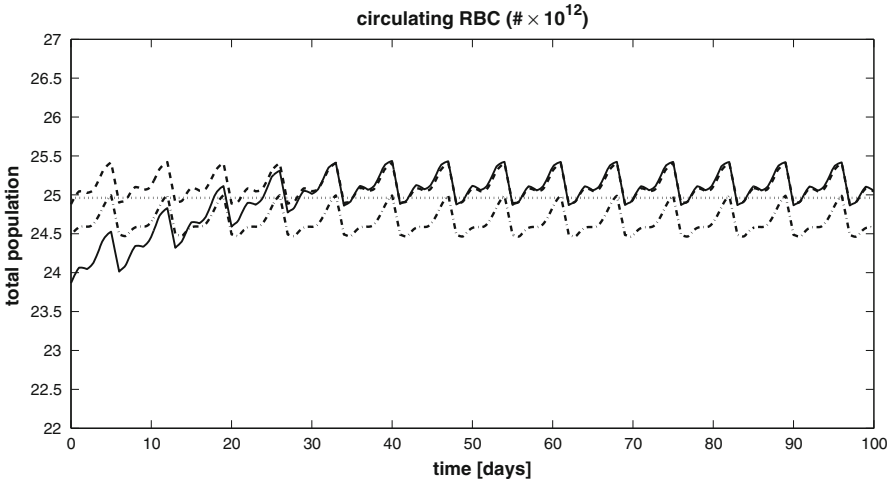

Fig. 12 Consequence of different life spans on the amount of Epoetin-α which has to be administered when in addition an increased loss of RBCs ($\gamma_r^m = 0.015$ instead of $\gamma_r^m = 0.005$) has to be considered. The *dotted line* represents the baseline for a healthy adult. Administration schemes: 2× per week; accumulated weekly dose and life span of RBCs: 15,000 U and 120 days (*solid line*), 18,000 U and 90 days (*dashed line*), 45,000 U and 60 days (*dash-dotted line*)

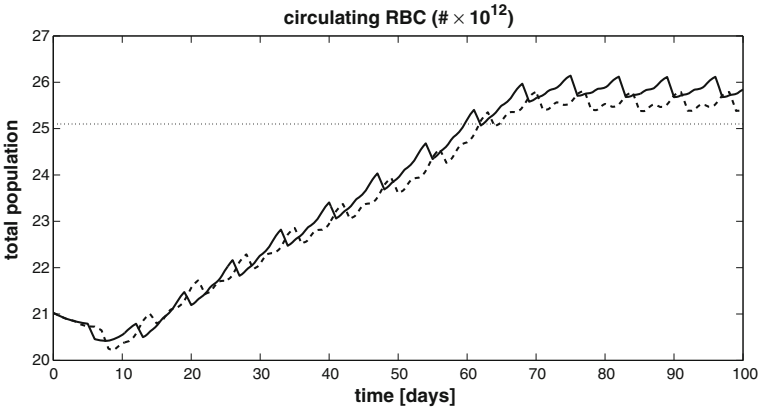

Fig. 13 Comparing a 2× per week (*dashed line*) and 3× per week (*solid line*) administration scheme for a dialysis patient without inflammation. The assumed average life span of the RBC is 60 days. The weekly dose accumulates to 15,000 U for the 2× per week scheme and to 9,000 U for the 3× per week scheme

is valid for modeling erythropoiesis in subjects whose erythropoietic iron demands are met. In addition, some situations where experimental data are not available were considered. Of particular interest are the implications of RBC lifespan for the choice of ESA dosing regimens (in this case Epoetin-α, see Figs. 11 and 12). Changes in the intrinsic mortality rate α_r^m (normal 0.005 per day, increased to 0.015, as for instance, in dialysis patients) were also considered. In each case, the endogenous EPO production was assumed to be reduced to the minor production by the liver, as would be the case, for example, for a dialysis patient. The dotted horizontal lines in Figs. 11, 12,

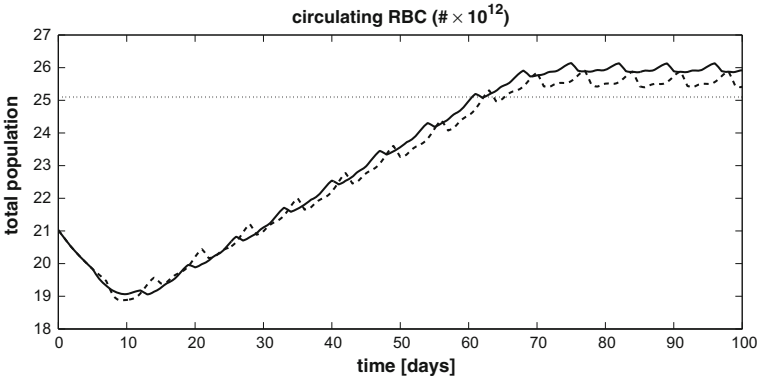

Fig. 14 Comparing a 2× per week (*dashed line*) and 3× per week (*solid line*) administration scheme for a dialysis patient without inflammation considering an increased loss of RBCs ($\gamma_r^m = 0.015$ instead of $\gamma_r^m = 0.005$). The assumed average life span of the RBCs is 60 days. The weekly dose accumulates to 50,000 U for the 2× per week scheme and to 15,000 U for the 3× per week scheme

Table 3 Comparisons of ESA administration schemes under varying conditions

Administration scheme	Intrinsic mortality rate α_r^m for RBCb (per day)	Life-span for RBC (days)	Dosage per administration (U)	Dosage per week (U)	Figure
2× per week	0.005	120	4,000	8,000	Fig. 11
2× per week	0.005	90	4,750	9,500	
2× per week	0.005	60	7,000	14,000	
2× per week	0.015	120	7,500	15,000	Fig. 12
2× per week	0.015	90	9,000	18,000	
2× per week	0.015	60	22,500	45,000	
2× per week	0.005	60	7,500	15,000	Fig. 13
3× per week	0.005	60	3,000	9,000	
2× per week	0.015	60	25,000	50,000	Fig. 14
3× per week	0.015	60	5,000	15,000	

Considered are different intrinsic mortality rates, different life spans for RBCs and administration of ESA 2 or 3 times a week

13, 14 indicate the baseline population sizes for a healthy subject ($\alpha_r^m = 0.005$ and life span for RBCs = 120 days). The simulations indicate a considerable increase of the administration dosages when life span of RBCs decreases, the rate α_r^m increases, and the frequency of administrations decreases (see Table 3 and Figs. 11, 12, 13, 14).

References

Ackleh AS, Banks HT, Deng K (2002) A finite difference approximation for a coupled system of nonlinear size-structured population. Nonlinear Anal 50:727–748

Ackleh AS, Deng K, Ito K, Thibodeaux J (2006) A structured erythropoiesis model with nonlinear cell maturation velocity and hormone decay rate. Math Biosci 204:21–48

Adimy M, Crauste F, Ruan S (2006) Modelling hematopoiesis mediated by growth factors with applications to periodic hematological diseases. Bull Math Biol 68:2321–2351
Alfrey CP, Fishbane S (2007) Implications of neocytolysis for optimal management of anaemia in chronic kidney disease. Nephron Clin Pract 106:149–156
Alfrey CP, Udden MM, Leach-Huntoon C, Driscoll T, Pickett MH (1996) Control of red blood cell mass in spaceflight. J Appl Physiol 81:98–104
Banks HT, Cole CE, Schlosser PM, Tran HT (2004) Modelling and optimal regulation of erythropoiesis subject to benzene intoxication. Math Biosci Eng 1:15–48
Barosi G, Cazzola M, Berzuini C, Quaglini S, Stefanelli M (1985) Classification of anemia on the basis of ferrokinetic parameters. Br J Haematol 61:357–370
Belair J, Mackey MC, Mahaffy JM (1995) Age-structured and two-delay models for erythropoiesis. Math Biosci 128:317–346
Besarab A, Bolton WK, Browne JK, Egrie JC, Nissenson AR, Okamoto DM, Schwab SJ, Goodkin DA (1998) The effects of normal as compared with low hematocrit values in patients with cardiac disease who are receiving hemodialysis and epoetin. New Engl J Med 339:584–590
Besarab A, Reyes CM, Hornberger J (2002) Meta-analysis of subcutaneous versus intravenous epoetin in maintenance treatment of anemia in hemodialysis patients. J Kidney Dis 40:439–446
Chang CC, Chen Y, Modi K, Awar OG, Alfrey CP, Rice L (2009) Changes of red blood cell surface markers in a blood doping model of neocytolysis. J Investig Med 57:650–654
Cheung W, Minton N, Gunawardena K (2001) Pharmocokinetics and pharmacodynamics of epoetin alfa once weekly and three times weekly. Eur J Clin Pharmacol 57:411–418
Crauste F, Pujo-Menjouet L, Genieys S, Molina C, Gandrillon O (2008) Adding self-renewal in committed erythroid progenitors improves the biological relevance of a mathematical model of erythropoiesis. J Theor Biol 250:322–338
Crichton R (2009) Iron metabolism: from molecular mechanisms to clinical consequences, 3rd edn. Wiley, New York
Feagan BG, Wong CJ, Kirkley A, Johnston DW, Smith FC, Whitsitt P, Wheeler S, Lau CY (2000) Erythropoietin with iron supplementation to prevent allogeneic blood transfusion in total hip joint arthroplasty. Ann Intern Med 133:845–854
Finch CA (1982) Erythropoiesis, erythropoietin, and iron. Blood The Journal of American Society of Hematology 60(6):1241–1246
Finch S, Haskins D, Finch CA (1950) Iron metabolism. Hematopoiesis following phlebotomy. Iron as a limiting factor. J Clin Investig 29:1078–1086
Fleming MD (2008) The regulation of hepcidin and its effects on systemic and cellular iron metabolism. Hematology Journal of American Society of Hematology 2008(1):151–158
Fowler WM, Barner AP (1942) Rate of hemoglobin regeneration in blood donors. J Am Med Assoc 118(6):421–427
Go AS, Chertow GM, Fan D, McCulloch CE, Hsu C (2004) Chronic kidney disease and the risks of death, cardiovascular events, and hospitalization. New Engl J Med 351:1296–1305
Goodnough LT (2002) The role of iron in erythropoiesis in the absence and presence of erythropoietin therapy. Nephrol Dial Transplant 17:14–18
Greer JP, Foerster J, Rodgers GM, Paraskevas F, Glader B, Arber DA, Means RTJ (2009) Wintrobe's clinical hematology, vol 1, 12th edn. Lippincott Williams and Wilkins, Philadelphia
Ito K, Kappel F (2002) Evolution equations and approximations. World Scientific, Singapore
Jandl JH (1987) Blood. Textbook of Hematology. Little, Brown and Company, Boston
Jaspan D (2007) Erythropoietic therapy: cost efficiency and reimbursement. Am J Health-System Pharm 64(16 Suppl 11):19–29. doi:10.2146/ajhp070246
Kappel F, Zhang K (1993) Approximation of linear age-structured population models using Legendre polynomials. J Math Anal Appl 180:518–549
Kotanko P, Kuhlmann MK, Levin NW (2007) Hemodialysis: technology, adequacy, and outcomes. In: Feehally J, Floege J, Johnson JR (eds) Comprehensive clinical nephrology, chap 83. Mosby Elsevier, Philadelphia, pp 953–966
Lichtman MA, Beutler E, Kipps TJ, Seligsohn U, Kaushansky K, Prchal JT (eds) (2005) Williams hematology, 7th edn. McGraw-Hill, New York
Loeffler M, Pantel K, Wulff H, Wichmann HE (1989) A mathematical model of erythropoiesis in mice and rats. Part 1. Structure of the model. Cell Tissue Kinetics 22:13–30

Mahaffy JM, Belair J, Mackey MC (1998) Hematopoietic model with moving boundary condition and state dependent delay: applications in erythropoiesis. J Theor Biol 190:135–146

Mahaffy JM, Polk SW, Roeder RK (1999) An age-structured model for erythropoiesis following a phlebotomy. Tech. Rep. CRM-2598, Department of Mathematical Sciences, San Diego State University, San Diego, CA 92182-0314

Pottgiesser T, Specker W, Umhau M, Dickhuth HH, Roecker K, Schumacher YO (2008) Recovery of hemoglobin mass after blood donation. Transfusion 48:1390–1397

Rice L, Alfrey CP (2005) The negative regulation of red cell mass by neocytolysis: physiologic and pathophysiologic manifestations. Cell Physiol Biochem 15:245–250

Rice L, Alfrey CP, Driscoll T, Whitley CE, Hachey DL, Suki W (1999) Neocytolysis contributes to the anemia of renal disease. Am J Kidney Dis 33:59–62

Rice L, Ruiz W, Driscoll T, Whitley CE, Tapia R, Hachey DL, Conzales GF, Alfrey CP (2001) Neocytolysis on descent from altitude: a newly recognized mechanism for the control of red cell mass. Ann Intern Med 134:652–656

Roeder I (2006) Quantitative stem cell biology: computational studies in the hematopoietic system. Curr Opin Hematol 13:222–228

Roeder I, Loeffler M (2002) A novel dynamic model of hematopoietic stem cell organization based on the concept of within-tissue plasticity. Exp Hematol 30:853–861

Schaefer RM, Schaefer L (1998) Iron monitoring and supplementation: how do we achieve the best results. Nephrol Dial Transplant 13:9–12

Stefanelli M, Bentley DP, Cavill I, Roeser HP (1984) Quantitation of reticuloendothelial iron kinetics in humans. Am J Physiol 247:842–849

Strippoli GF, Craig JC, Manno C, Schena FP (2004) Hemoglobin targets for the anemia of chronic kidney disease: a meta-analysis of randomized, controlled trials. J Am Soc Nephrol 15:3154–3165

Udden MM, Driscoll TB, Pickett MH, Leach-Huntoon CS, Alfrey CP (1995) Decreased production of red blood cells in human subjects exposed to microgravity. J Lab Clin Med 125:442–449

Wichmann HE, Loeffler M, Pantel K, Wulff HH (1989) A mathematical model of erythropoiesis in mice and rats. Part 2. Stimulated erythropoiesis. Cell Tissue Kinetics 22:31–49

Wu H, Liu X, Jaenisch R, Lodish HF (1995) Generation of committed erythroid BFU-E and CFU-E progenitors does not require erythropoietin or the erythropoietin receptor. Cell 83(1):59–67

Wulff H, Wichmann HE, Pantel K, Loeffler M (1989) A mathematical model of erythropoiesis in mice and rats. Part 3: suppressed erythropoiesis. Cell Tissue Kinetics 22:51–61